The Nature of the Hydrogen Bond in DNA Base Pairs:
The Role of Charge Transfer and Resonance Assistance

Célia Fonseca Guerra,[b] F. Matthias Bickelhaupt,*[a] Jaap G. Snijders,[c] and Evert Jan Baerends[b]

Abstract: The view that the hydrogen bonds in Watson – Crick adenine – thymine (AT) and guanine – cytosine (GC) base pairs are in essence electrostatic interactions with substantial resonance assistance from the π electrons is questioned. Our investigation is based on a state-of-the-art density functional theoretical (DFT) approach (BP86/TZ2P) that has been shown to properly reproduce experimental data. Through a quantitative decomposition of the hydrogen bond energy into its various physical terms, we demonstrate that, contrary to the widespread belief, donor – acceptor orbital interactions (i.e., charge transfer) in σ symmetry between N or O lone pairs on one base and N−H σ*-acceptor orbitals on the other base do provide a substantial bonding contribution which is, in fact, of the same order of magnitude as the electrostatic interaction term. The overall orbital interactions are reinforced by a small π component which stems from polarization in the π-electron system of the individual bases. This π component is, however, one order of magnitude smaller than the σ term. Furthermore, we have investigated the synergism in a base pair between charge transfer from one base to the other through one hydrogen bond and in the opposite direction through another hydrogen bond, as well as the cooperative effect between the donor – acceptor interactions in the σ- and polarization in the π-electron system. The possibility of C−H···O hydrogen bonding in AT is also examined. In the course of these analyses, we introduce an extension of the Voronoi deformation density (VDD) method which monitors the redistribution of the σ- and π-electron densities individually out of ($\Delta Q > 0$) or into ($\Delta Q < 0$) the Voronoi cell of an atom upon formation of the base pair from the separate bases.

Keywords: charge transfer · density functional calculations · DNA structures · hydrogen bonds · resonance assistance

Introduction

Although it is the weakest chemical interaction, the hydrogen bond plays a key role in the chemistry of life.[1] Apart from providing water with physical properties that make it the ideal medium for many processes of life to take place in, it is responsible for various types of self-organization and molecular recognition, such as the folding of proteins. As proposed already in 1953 by Watson and Crick,[1c] hydrogen bonds are also essential to the working of the genetic code contained in DNA.[1] The latter consists of two helical chains of nucleotides which are held together by the hydrogen bonds that arise between a purine- and a pyrimidine-derived nucleic base. In particular, this base pairing occurs specifically between adenine (A, a purine) and thymine (T, a pyrimidine), and between guanine (G, a purine) and cytosine (C, a pyrimidine), giving rise to the so-called Watson – Crick AT and GC pairs (Scheme 1).

In the past decade, ab initio and DFT quantum chemical studies[2] have appeared on the geometry, energy and other aspects of the hydrogen bonds that hold together AT and GC pairs. The adequacy of DFT for hydrogen-bonded systems has received much attention lately.[3] It is known from the investigations of Sim et al.[3a] on the water dimer and the formamide – water complex that DFT with nonlocal gradient corrections is capable of describing hydrogen-bonded systems reasonably well. They found that the DFT results are of comparable quality to those from correlated ab initio methods. Others[2e,j–l] have shown that this is also true for the strength of hydrogen bonds in DNA base pairs, while for the corresponding structures minor but significant deviations

[a] Dr. F. M. Bickelhaupt
Fachbereich Chemie der Philipps-Universität
Hans-Meerwein-Strasse, D-35032 Marburg (Germany)
Fax: (+49) 6421 28 28917
E-mail: bickel@chemie.uni-marburg.de

[b] Dr. C. Fonseca Guerra, Prof. Dr. E. J. Baerends
Afdeling Theoretische Chemie
Scheikundig Laboratorium der Vrije Universiteit
De Boelelaan 1083, NL-1081 HV Amsterdam (The Netherlands)

[c] Prof. Dr. J. G. Snijders
Theoretische Chemie, Rijksuniversiteit Groningen
Nijenborgh 4, NL-9747 AG Groningen (The Netherlands)

Adenine–Thymine

Guanine–Cytosine
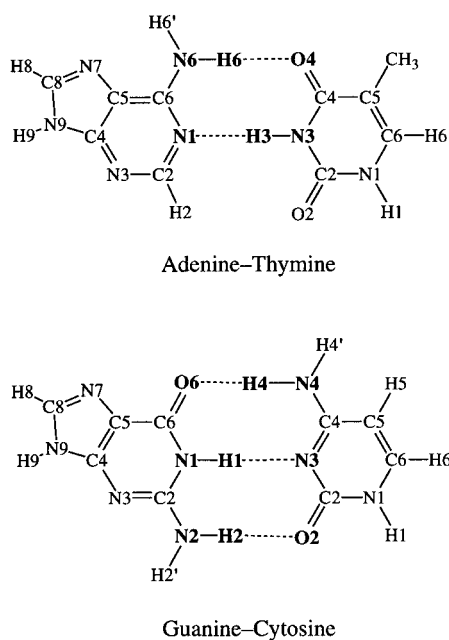
Scheme 1. Nomenclature used throughout this work.

Abstract in German: *Die Auffassung, daß die Wasserstoff-brücken in den Watson–Crick-Basenpaaren Adenin–Thymin (AT) und Guanin–Cytosin (GC) im wesentlichen auf elektrostatischen Wechselwirkungen beruhen mit einer substanziellen Unterstützung durch Resonanz im π-System, wird in Frage gestellt. Unsere Untersuchungen beruhen auf einem modernen dichtefunktionaltheoretischen (DFT) Ansatz (BP86/TZ2P), der die experimentellen Daten korrekt reproduziert. Mittels einer quantitativen Zerlegung der Wasserstoffbrücken-Bindungsenergie in ihre verschiedenen physikalischen Terme zeigen wir, daß entgegen der gängigen Auffassung Donor/Akzeptor-Orbitalwechselwirkungen (d. h. Ladungstransfer) in σ-Symmetrie zwischen einsamen Elektronenpaaren am N oder O der einen Base und N—H σ*-Akzeptororbitalen der anderen Base einen substanziellen Beitrag zur Bindung liefern, welcher tatsächlich von der gleichen Größenordnung wie die elektrostatische Wechselwirkung ist. Insgesammt werden die Orbital-wechselwirkungen verstärkt durch eine kleine π-Komponente, welche von der Polarisation des π-Elektronensystems der einzelnen Basen stammt. Diese π-Komponente ist jedoch eine Größenordnung kleiner als der σ-Term. Ferner untersuchten wir den Synergismus innerhalb eines Basenpaares zwischen Ladungstransfer von der einen zur anderen Base über eine Wasserstoffbrücke und in die entgegengesetzte Richtung über eine andere Wasserstoffbrücke, wie auch den kooperativen Effekt zwischen Donor/Akzeptor-Wechselwirkungen im σ-System und Polarisation im π-Elektronensystem. Auch die Möglichkeit einer C—H · · · O-Wasserstoffbrücke in AT wurde in Betracht gezogen. Im Rahmen dieser Analysen führen wir eine Erweiterung der Voronoi-Deformationsdichte- (VDD) Methode ein, welche die mit der Bildung des Basenpaars aus den separaten Basen verbundene Umverteilung von σ- und π-Electronendichte aus der Voronoi-Zelle ($\Delta Q > 0$) oder in die Voronoi-Zelle ($\Delta Q < 0$) eines jeden Atoms wiedergibt.*

from experimental values were obtained with both DFT and ab initio methods. Very recently, we[4, 5] have shown that these structural deviations are a result of intermolecular interactions of the base pairs with the environment in the crystal. These discrepancies can be resolved if the most important environment effects are incorporated into the model system, yielding DFT structures for DNA base pairs in excellent agreement with experiment.[4, 5]

For a true comprehension of the structure, properties and behavior of DNA base pairs, a sound understanding of the hydrogen bonds involved is indispensable. Yet, its nature is not at all clear. The importance, for example, of covalence in these hydrogen bonds, that is the magnitude of donor–acceptor orbital interactions, is still unknown. Based on the work of Umeyama and Morokuma[6] on dimers and codimers of HF, H_2O, NH_3 or CH_4, weak and medium range hydrogen bonds are generally believed to be predominantly electrostatic in nature. On the other hand, Gilli et al.[7] suggested that the relatively strong hydrogen bonds in DNA base pairs cannot be understood solely on the basis of electrostatic interactions. In their work on β-diketone enols,[7a,c] they ascribed the strong intra- and intermolecular hydrogen bonds found in the corresponding monomers and dimers to a phenomenon, first appreciated by Huggins,[8] that they designated resonance-assisted hydrogen bonding (RAHB): Resonance in the π system assists the hydrogen bond by making the proton-acceptor more negative and the proton-donor more positive. Because of the close similarity between the hydrogen-bonding patterns in β-diketone enols (monomers and dimers) and those in DNA base pairs—both involve hydrogen bonds between proton-acceptor and proton-donor atoms that are connected through a conjugated π system—they suggested that "nature itself may have taken advantage of the greater energy of RAHB to keep control of molecular associations whose stability is essential for life".

In this work, we try to clarify the nature of the hydrogen bonds in the Watson–Crick DNA base pairs with nonlocal density functional theory (DFT). In the conceptual framework provided by Kohn–Sham molecular orbital (KS-MO) theory,[9] we investigated the hydrogen-bonding mechanism through an analysis of the electronic structure and a quantitative decomposition of the bond energy into the electrostatic interaction, the repulsive orbital interactions (Pauli repulsion) and the bonding orbital interactions (charge transfer and polarization). This enables us to address a number of fundamental questions. How important are electrostatics and charge transfer really? And, is there a synergism between charge transfer from one base to the other through one hydrogen bond, and in the opposite direction through another hydrogen bond? In other words, does the overall hydrogen-bond strength benefit from this mechanism that reduces the net build-up of charge on a base caused by the individual hydrogen bonds? Furthermore, we tried to find evidence for the resonance-assisted hydrogen bonding proposed by Gilli et al.[7a] and we test the hypothesis[10] of C—H · · · O hydrogen bonding in the AT base pair.

Complementary to the analysis of the orbital electronic structure, we have also studied the electronic density of the DNA bases and, in particular, how this is affected by the

formation of the hydrogen bonds in the base pairs. For this purpose, we have developed two extensions to the Voronoi deformation density (VDD) method:[11] i) A scheme for computing changes in the atomic charges of a polyatomic fragment as a result of the chemical interaction with another fragment, and ii) a partitioning of these changes in atomic charges into the contributions from different irreducible representations. These new features in VDD enable us to compute the change in σ and π density in the Voronoi cell of a particular atom as a result of the DNA base-pairing interaction.

Theoretical Methods

General procedure: All calculations were performed with the Amsterdam density functional (ADF) program[12] developed by Baerends et al.,[12a–d] vectorized by Ravenek,[12e] and parallelized[12a] as well as linearized[12f] by Fonseca Guerra et al. The numerical integration was performed with the procedure developed by te Velde et al.[12g,h] The MOs were expanded in a large uncontracted set of Slater type orbitals (STOs) containing diffuse functions: TZ2P (no Gaussian functions are involved).[12i] The basis set is of triple-ζ quality for all atoms and has been augmented with two sets of polarization functions, that is 3d and 4f on C, N, O, and 2p and 3d on H. The 1s core shell of carbon, nitrogen and oxygen were treated by the frozen-core approximation.[12b] An auxiliary set of s, p, d, f, and g STOs was used to fit the molecular density and to represent the Coulomb and exchange potentials accurately in each self-consistent field cycle.[12j]

Geometries and energies were calculated with nonlocal density functionals (NL). Equilibrium structures were optimized by using analytical gradient techniques.[12k] Frequencies[12l] were calculated by numerical differentiation of the analytical energy gradients with the nonlocal density functionals.

Exchange is described by Slater's $X\alpha$ potential[12m] with corrections from Becke[12n,o] added self consistently and correlation is treated in the Vosko–Wilk–Nusair (VWN) parametrization[12p] with nonlocal corrections by Perdew[12q] added, again, self consistently (BP86).[12r]

Bond enthalpies at 298.15 K and 1 atm (ΔH_{298}) were calculated from 0 K electronic bond (ΔE) according to Equation (1), assuming an ideal gas.[13]

$$\Delta H_{298} = \Delta E + \Delta E_{trans,298} + \Delta E_{rot,298} + \Delta E_{vib,0} + \Delta(\Delta E_{vib})_{298} + \Delta(pV) \quad (1)$$

Here, $\Delta E_{trans,298}$, $\Delta E_{rot,298}$ and $\Delta E_{vib,0}$ are the differences between products and reactants in translational, rotational, and zero point vibrational energy, respectively; $\Delta(\Delta E_{vib})_{298}$ is the change in the vibrational energy difference from 0 to 298.15 K. The vibrational energy corrections are based on our frequency calculations. The molar work term $\Delta(pV)$ is $(\Delta n)RT$; $\Delta n = -1$ for two fragments combining to one molecule. Thermal corrections for the electronic energy are neglected. The basis set superposition error (BSSE), associated with the hydrogen bond energy, has been computed by

the counterpoise method,[14] by using the individual bases as fragments.

Bonding energy analysis: The bonding in the AT and GC systems was analyzed with the extended transition state (ETS) method developed by Ziegler and Rauk.[15] The overall bond energy ΔE is made up of two major components [Eq. (2)].

$$\Delta E = \Delta E_{prep} + \Delta E_{int} \quad (2)$$

In Equation (2) the preparation energy ΔE_{prep} is the amount of energy required to deform the separate bases from their equilibrium structure to the geometry that they acquire in the base pair. The interaction energy ΔE_{int} corresponds to the actual energy change when the prepared bases are combined to form the base pair. The interaction energy is further split up into three physically meaningful terms [Eq. (3)].

$$\Delta E_{int} = \Delta V_{elstat} + \Delta E_{Pauli} + \Delta E_{oi} \quad (3)$$

The term ΔV_{elstat} corresponds to the classical electrostatic interaction between the unperturbed charge distributions of the prepared (i.e., deformed) bases and is usually attractive. The Pauli-repulsion ΔE_{Pauli} comprises the destabilizing interactions between occupied orbitals and is responsible for the steric repulsion. The orbital interaction ΔE_{oi} accounts for charge transfer (interaction between occupied orbitals on one moiety with unoccupied orbitals of the other, including the HOMO–LUMO interactions) and polarization (empty/occupied orbital mixing on one fragment). It can be decomposed into the contributions from each irreducible representation Γ of the interacting system [Eq. (4)].[15] In systems with a clear σ, π separation (like our DNA base pairs), this symmetry partitioning proves to be most informative.

$$\Delta E_{oi} = \sum_{\Gamma} \Delta E_{\Gamma} \quad (4)$$

Results and Discussion

Geometry and hydrogen bond strength

The results of our BP86/TZ2P study on the formation of the adenine–thymine and guanine–cytosine complexes are summarized and compared with literature in Tables 1 (energies), 2 and 3 (geometries). Scheme 1 defines the proton donor–acceptor distances used throughout this work. The structures calculated in C_1 point group symmetry, without any symmetry

Table 1. Hydrogen bond energies [kcal mol^{-1}] of AT and GC.[a]

Base	ΔE	ΔE_{BSSE}	ΔH_{298}	ΔH_{exp}
AT[b]	− 13.0	− 12.3	− 11.8	− 12.1[d]
AT[c]	− 13.0	− 12.3		
GC[b]	− 26.1	− 25.2	− 23.8	− 21.0[d]
GC[c]	− 26.1	− 25.2		

[a] BP86/TZ2P. ΔE and ΔE_{BSSE} are the bond energy at zero K without and with correction for the BSSE, respectively. ΔH_{298} is the bond enthalpy at 298 K. [b] Full optimization of base pair and separate bases. [c] Base pair optimized in C_s symmetry; full optimization of separate bases. [d] ΔH_{exp}, experimental ΔH from mass spectrometry data[18] with corrections for AT according to Brameld et al.[2i]

Table 2. Distances [Å] between proton-donor and acceptor atoms of AT.[a]

Level of theory	N6(H)⋯O4	N1⋯(H)N3
BP86/TZ2P[b]	2.85	2.81
BP86/TZ2P[c]	2.85	2.81
HF/6-31G**[c,d]	3.09	2.99
HF/cc-pVTZ(-f)[b,e]	3.06	2.92
B3LYP/6-31G**[b,f]	2.94	2.84

[a] BP86/TZ2P. See Scheme 1. [b] Full optimization in C_1 symmetry. [c] Optimized in C_s symmetry. [d] Sponer et al.[2e] [e] Brameld et al.[2i] [f] Bertran et al.[2l]

Table 3. Distances [Å] between proton-donor and acceptor atoms of GC.[a]

Level of theory	N2(H)⋯O2	N1(H)⋯N3	O6⋯(H)N4
BP86/TZ2P[b]	2.87	2.88	2.73
BP86/TZ2P[c]	2.87	2.88	2.73
HF/6-31G**[c,d]	3.02	3.04	2.92
HF/cc-pVTZ(-f)[b,e]	2.92	2.95	2.83
B3LYP/6-31G**[b,f]	2.92	2.93	2.79

[a] BP86/TZ2P. See Scheme 1. [b] Full optimization in C_1 symmetry. [c] Optimized in C_s symmetry. [d] Sponer et al.[2e] [e] Brameld et al.[2i] [f] Bertran et al.[2l]

constraints, were confirmed to be energy minima through a vibrational analysis that revealed zero imaginary frequencies. The choice for the BP86 density functional[12n–q] is based on our investigation[5] on the performance of various nonlocal density functionals for these systems which showed that BP86 agrees slightly better with experiment than PW91[16] and BLYP.[12o, 17]

The computed BP86/TZ2P bond enthalpies for the AT and GC pairs of -11.8 and -23.8 kcal mol^{-1} agree well with the experimental results of -12.1 and -21.0 kcal mol^{-1},[18] deviating by as little as $+0.3$ and -2.8 kcal mol^{-1}, respectively (see Table 1). The basis set superposition error (BSSE) of some 0.7 kcal mol^{-1} is quite small. An important point is that there is essentially no difference between both geometries and bond energies associated with DNA bases and base pairs optimized in C_s symmetry, and those obtained in C_1 symmetry, that is without any symmetry restrictions. The various hydrogen-bond lengths in AT and GC, that is the distances between the proton-donor and proton-acceptor atoms, differ by less than 0.01 Å (see Tables 2 and 3). Likewise, the formation of C_s-symmetric base pairs (again from fully optimized bases) yields bond energies ΔE that differ by less than 0.1 kcal mol^{-1} from those for the same process without symmetry constraint (see Table 1). As a consequence, we may analyze the A–T and G–C bonding mechanisms in C_s symmetry, thus enabling us to decompose the orbital interactions into a σ and a π component [Eq. (4)].

As mentioned in our communication[4] and further investigated in ref. [5], gas-phase theoretical geometries can not be directly compared with experimental X-ray crystal structures[1d, 19] that are subjected to and influenced by packing forces as well as intermolecular interactions. Therefore, in the present study, we restrict ourselves to a brief comparison between our results and those from a few other theoretical studies (for an exhaustive comparison with other theoretical[2d,e,i,k,l] and experimental[1d, 19] studies, see ref. [5]). The Hartree–Fock approach (HF/6-31G**)[9, 13] yields distances

that are up to 0.2 Å longer than our BP86/TZ2P values. The agreement between our distances and those obtained by Bertran et al.[2l] at B3LYP/6-31G** is better, the latter being only up to 0.1 Å longer than ours. The remaining variance is probably not only due to the different functionals but also the different basis sets as well as technical differences between the programs used.

The deformation of the bases (i.e., changes in bond lengths larger than 0.1 Å) caused by the formation of the hydrogen bonds is shown in Figure 1. All the N–H bonds that participate in hydrogen bonding expand by 0.02–0.05 Å. The largest elongations are found for the N3–H3 of thymine ($+0.05$ Å) and the N4–H4 of cytosine ($+0.04$ Å). The C=O distances of oxygen atoms involved in hydrogen bonding increase by some 0.02 Å. Furthermore, we see that G–C base pairing leads to somewhat stronger distortions of the corresponding bases than A–T base pairing. In the next section, we will explain how charge-transfer interactions in the σ system and polarization in the π system are responsible for these deformations.
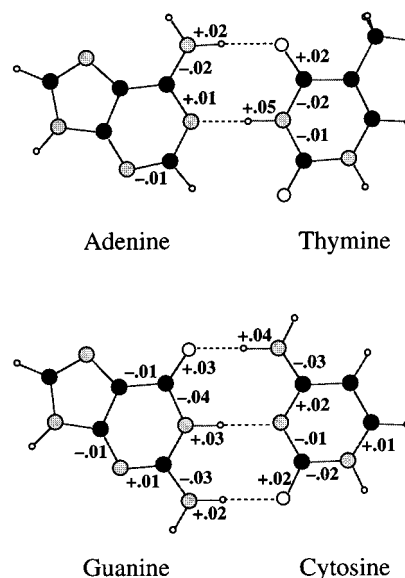

Figure 1. Deformation [Å] of the individual bases caused by hydrogen bonding in the base pairs, from BP86/TZ2P optimizations without any symmetry constraint (only changes in bond length ≥ 0.01 Å are given).

Nature of the hydrogen bond

Electronic structure of DNA bases: In order to form stable base pairs, DNA bases must be structurally and electronically complementary. The role of structural complementarity has been discussed very recently by Kool and others.[20] Here, we focus on the electronic structure of the four DNA bases and their capability to form stable A–T and G–C hydrogen bonds. First, we examine if the bases do possess the right charge distribution for achieving a favorable electrostatic interaction in the Watson–Crick base pairs. This turns out to be the case, as can be seen from Figure 2, which displays the VDD atomic charges[11] (see also section on charge distribution) for the separate, noninteracting bases: All proton-acceptor atoms have a negative charge whereas the corresponding protons they face are all positively charged.
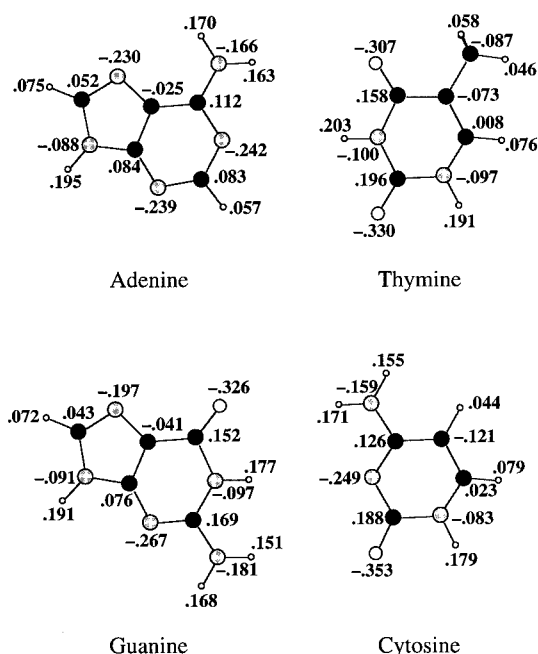
Figure 2. VDD atomic charges [electrons] of the isolated bases adenine, thymine, guanine and cytosine obtained at BP86/TZ2P (see Scheme 1).

Next, we consider the possibility of charge-transfer interactions in the σ-electron system. Scheme 2 displays the basic features in the electronic structures that are required in order for these donor–acceptor orbital interactions to occur: A lone pair on a nitrogen or oxygen atom of one base pointing toward (and donating charge into) the unoccupied σ* orbital of an N–H group of the other base; this leads to the formation of a weak $\sigma_{LP} + \sigma^{*}_{N-H}$ bond.
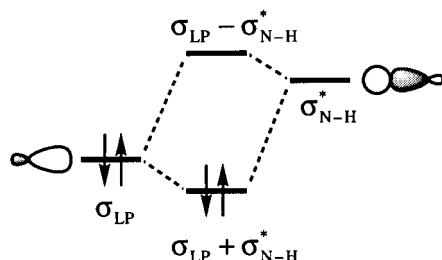
Scheme 2. Donor–acceptor orbital interaction.

Of course, the electronic structure and bonding mechanism in DNA base pairs, with two or three hydrogen-bonding contacts occurring simultaneously, are somewhat more complicated. Not only the HOMOs and LUMOs of the σ-electron system but also some of the other high-energy occupied and low-energy unoccupied orbitals of the bases are involved in frontier-orbital interactions. However, the basic bonding pattern should still be that of Scheme 2: The occupied orbitals at high energy must have lone-pair character on the charge-donating nitrogen or oxygen atoms and the unoccupied orbitals at low energy must be σ* antibonding on the charge-accepting N–H group (vide infra). Indeed, as can be seen from the contour plots of the DNA-base frontier orbitals

in Figures 3 and 4—and anticipating the outcome of our orbital-interaction analyses—this turns out to be the case.

We begin with the bases of the AT pair (see Figure 3). Adenine has two occupied orbitals, the σ_{HOMO-1} and the σ_{HOMO}, that have lone-pair-like lobes on the nitrogen atoms N1, N3 and N7 (see also Scheme 1). Through their lobe on N1, they can overlap with and donate charge into the lowest unoccupied orbitals of thymine which all have N3–H3 σ* character (they have also σ* character on C–H and other N–H groups of thymine but this is of no direct importance for A–T bonding); one of these thymine acceptor orbitals, the σ_{LUMO+1}, is shown in Figure 3. Likewise, the σ_{HOMO-1} and σ_{HOMO} of thymine are essentially lone pairs on the oxygen atoms O2 and O4. With their lobe on O4, they can overlap and interact with the complementary N6–H6 σ*-antibonding virtuals on adenine, e.g. the σ_{LUMO} (Figure 3).
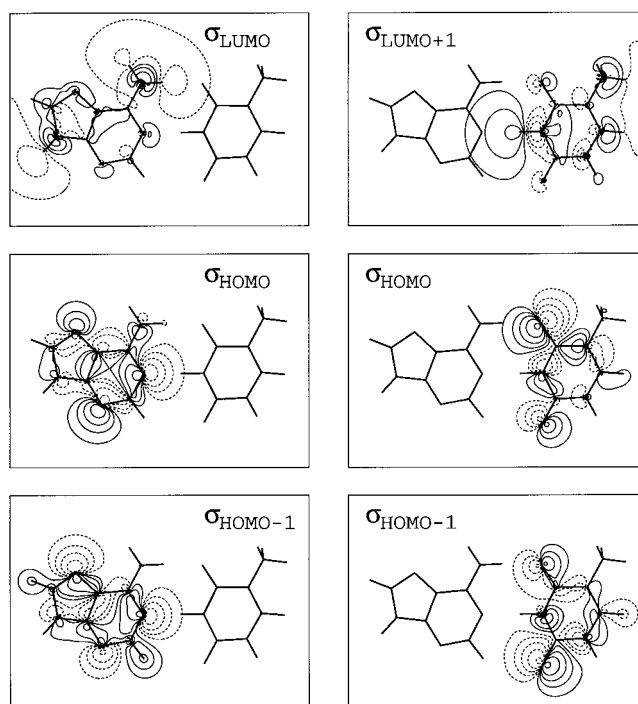

Figure 3. Contour plots of the σ_{HOMO-1}, σ_{HOMO} and σ_{LUMO} of adenine and the σ_{HOMO-1}, σ_{HOMO} and σ_{LUMO+1} of thymine obtained at BP86/TZ2P (Scan values: ±0.5, ±0.2, ±0.1, ±0.05, ±0.02. Solid and dashed contours refer to positive and negative values, respectively). For each fragment molecular orbital (FMO), both its own base and the other base in the Watson–Crick pair are shown as wire frames.

The situation for the bases of the GC pair is very similar (see Figure 4). The σ_{HOMO} of guanine is basically a lone pair on O6 that points toward and can donate charge into the lowest unoccupied orbitals of cytosine that have N4–H4 σ*-antibonding character, e.g. the σ_{LUMO} (Figure 4). The σ_{HOMO-1} and σ_{HOMO} of cytosine are a lone pair on N3 and O2, respectively. They can overlap and interact with the lowest unoccupied orbitals on guanine with N1–H1 and N2–H2 σ*-antibonding character. Interestingly, the σ_{LUMO}, the σ_{LUMO+2} (not shown in Figure) and the σ_{LUMO+3} of guanine can be conceived as the totally bonding (plus–plus–plus), the nonbonding (plus–null–minus) and the antibonding (plus–
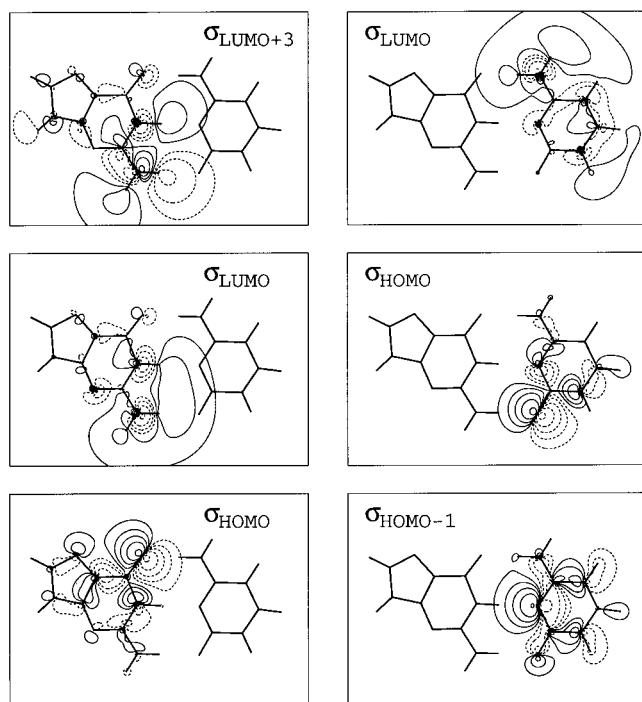
Figure 4. Contour plots of the σ_{HOMO}, σ_{LUMO} and σ_{LUMO+3} of guanine and σ_{HOMO-1}, σ_{HOMO} and σ_{LUMO} of cytosine obtained at BP86/TZ2P (see also legend to Figure 3).

Table 4. Overlaps between σ frontier orbitals of DNA bases in AT and GC.[a]

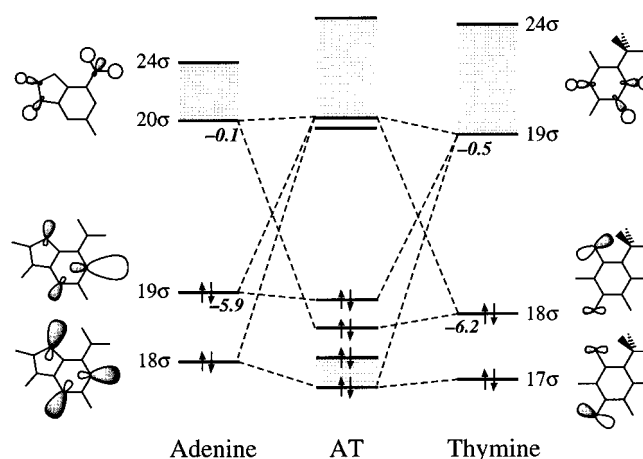| $\langle \sigma_A^{occ} \mid \sigma_T^{virt} \rangle$	$\mid 19\sigma_T \rangle$	$\mid 20\sigma_T \rangle$	$\mid 21\sigma_T \rangle$	$\mid 22\sigma_T \rangle$	$\mid 24\sigma_T \rangle$
$\langle 18\sigma_A \mid$	0.06	0.16	0.12	0.08	0.06
$\langle 19\sigma_A \mid$	0.08	0.19	0.14	0.09	0.06
$\langle \sigma_T^{occ} \mid \sigma_A^{virt} \rangle$	$\mid 20\sigma_A \rangle$	$\mid 21\sigma_A \rangle$	$\mid 22\sigma_A \rangle$	$\mid 23\sigma_A \rangle$	$\mid 24\sigma_A \rangle$
$\langle 18\sigma_T \mid$	0.08	0.07	0.04	0.03	0.09
$\langle \sigma_G^{occ} \mid \sigma_C^{virt} \rangle$	$\mid 17\sigma_C \rangle$	$\mid 18\sigma_C \rangle$	$\mid 19\sigma_C \rangle$	$\mid 20\sigma_C \rangle$	$\mid 21\sigma_C \rangle$
$\langle 20\sigma_G \mid$	0.003	0.002	0.005	0.003	0.005
$\langle 21\sigma_G \mid$	0.08	0.06	0.09	0.08	0.04
$\langle \sigma_C^{occ} \mid \sigma_G^{virt} \rangle$	$\mid 22\sigma_G \rangle$	$\mid 24\sigma_G \rangle$	$\mid 25\sigma_G \rangle$	$\mid 27\sigma_G \rangle$	
$\langle 15\sigma_C \mid$	0.22	0.24	0.16	0.04	
$\langle 16\sigma_C \mid$	0.15	0.03	0.09	0.02	

[a] BP86/TZ2P.

Figure 5. Diagram for the donor–acceptor interactions in the N6(H)⋯O4 and N1⋯(H)N3 hydrogen bonds between adenine and thymine with σ_{HOMO} and σ_{LUMO} energies [eV], obtained at BP86/TZ2P (the lowest unoccupied orbitals that participate in these interactions are represented by a block).

minus–plus) combinations, respectively, of the three N–H σ* orbitals corresponding to the N2–H2′, N2–H2 and N1–H1 groups.

A–T orbital interactions: Now, let us analyze how the frontier orbitals of the bases really interact in the Watson–Crick base pairs. Figures 5 and 6 show schematically the resulting MO diagrams for the σ-electron systems; relevant overlaps between occupied and virtual frontier orbitals are given in Table 4. The Kohn–Sham MO analyses of the A–T and G–C base-pairing interactions do indeed yield the bonding mechanism that we expected on the basis of the above qualitative considerations on the character and shape of the DNA-base orbitals. The picture is only complemented by a few repulsive four-electron orbital interactions that we did not consider above.

For AT, we find charge-transfer hydrogen bonding from A to T, through N1⋯H3–N3, and the other way around from T to A, through N6–H6⋯O4. The N1⋯H3–N3 bond arises from the donor–acceptor interaction between the two σ_{HOMO-1} and σ_{HOMO} nitrogen lone-pair orbitals of adenine (18σ and 19σ in Figure 5) and the lowest unoccupied N3–H3 σ* orbitals of thymine (19σ through 24σ, represented as a block in Figure 5). The N6–H6⋯O4 bond, donating charge in the opposite direction, is provided by the interaction between the σ_{HOMO} oxygen lone-pair orbital of thymine (i.e., 18σ) and the lowest unoccupied N6–H6 σ* orbitals of adenine (i.e., 20σ through 24σ, represented as a block in Figure 5). In addition, there is a repulsive orbital interaction between the σ_{HOMO-1} of adenine and the σ_{HOMO-1} of thymine, with a mutual orbital overlap of 0.19, which splits the A–T bonding combination of the adenine 18σ with the thymine 19σ through 24σ into the

σ_{HOMO-3} and σ_{HOMO-2} of the AT base pair; this "split orbital level" is represented as a block in the MO diagram. It is the donation of charge into the N–H antibonding σ* orbitals of adenine and thymine that is responsible for the slight elongation observed for the N–H bonds involved in hydrogen bonding (see Figure 1). The adenine σ_{LUMO}, σ_{LUMO+2} and σ_{LUMO+3}, for example, acquire populations of 0.05, 0.03, and 0.03 electrons, respectively (not shown in Table). The thymine σ_{LUMO} through σ_{LUMO+3} and σ_{LUMO+5} each gain 0.02 electrons. Also other deformations that occur upon base pairing are caused by these charge-transfer interactions in the σ-electron system but also by polarization (i.e., occupied–empty mixing of orbitals on the same base) in the π-electron system (vide infra).

As follows from the total VDD charges of the individual DNA bases in the Watson–Crick base pairs in Table 5, the charge-transfer from A to T associated with the N1⋯H3–N3 bond is stronger than that back from T to A through the N6–H6⋯O4 bond. This leads to an accumulation of negative charge of -0.03 electrons on thymine. Two factors are responsible for this build-up of charge. In the first place, the N1⋯H3–N3 bond comprises two donor orbitals on adenine

Table 5. Total charge transfer [electrons] between the individual DNA bases in Watson–Crick base pairs calculated with the extensions of the VDD method.[a]

	Adenine	Thymine	Guanine	Cytosine
$\Delta Q^{\sigma}_{total}$	0.03	− 0.03	− 0.03	0.03
ΔQ^{π}_{total}	0.00	0.00	0.00	0.00
ΔQ_{total}	0.03	− 0.03	− 0.03	0.03
σ virtuals on T and C only, no π virtuals at all[b]				
$\Delta Q^{\sigma}_{total}$	0.05	− 0.05	0.05	− 0.05
σ virtuals on A and G only, no π virtuals at all[c]				
$\Delta Q^{\sigma}_{total}$	− 0.04	0.04	− 0.07	0.07

[a] BP86/TZ2P. [b] Only charge transfer from A to T and from G to C possible. [c] Only charge transfer from T to A and from C to G possible.

for charge transfer into virtuals of thymine, whereas only one donor orbital on thymine is involved in the N6–H6···O4 bond for charge transfer back into virtuals on adenine. Secondly, the overlaps between the donor orbitals of adenine (18σ and 19σ) and the lowest unoccupied acceptor orbitals of thymine (19σ through 24σ) are with values of 0.06–0.19 significantly larger than those between the donor orbital of thymine and the acceptor orbitals of adenine that amount to 0.03–0.09 (see Table 4).

Note that the π-electron density does not contribute to the net A–T charge transfer ($\Delta Q^{\pi}_{total} = 0$, Table 5) which is thus entirely a result of the σ-orbital interactions. The absence of A–T charge transfer in the π-electron system is due to the extremely small π-orbital overlaps (in the order of 10^{-3}), which are one to two orders of magnitude smaller than those occurring between σ orbitals. There is however occupied–virtual mixing within the π system of each individual base. This is ascribed mainly to the electrostatic potential that one base experiences from the other base. This π polarization is responsible for a sizeable charge reorganization as discussed in the section on charge redistribution.

We have also tried to infer the amount of charge transfer associated with the individual N1···H3–N3 and N6–H6···O4 hydrogen bonds by removing either the σ virtuals from thymine (switching off N1···H3–N3) or from adenine (switching off N6–H6···O4) while at the same time all π virtuals are removed from both DNA bases (switching off polarization of the π electrons; see also last section on synergy in hydrogen bonding). The results (entries 4 and 5 in Table 5) confirm that more charge is transferred from A to T through N1···H3–N3 (0.05 electrons) than back from T to A through N6–H6···O4 (0.04 electrons). Note, however, that the difference between the amount of charge transferred in opposite directions through either of the two hydrogen bonds is somewhat smaller without (0.01 electrons, i.e., the difference between entries 4 and 5 in Table 5) than with all other interfering orbital interactions (0.03 electrons, see entry 1 in Table 5).

C–H···O hydrogen bonding in AT? Leonard et al.[10a] suggested that there is also a hydrogen bond between the C2–H2 bond of adenine and the oxygen atom O2 of thymine that would contribute to the stability of the AT pair. However, our analyses show that this is not the case. In the first place, already the distance between this C–H bond and O atom is

too large to be indicative for a hydrogen-bonding interaction (C2–O2 = 3.63 Å and H2–O2 = 2.81 Å). But more importantly, we did not find any donor–acceptor orbital interaction corresponding with a C2–H2···O2 bond. Accordingly, neither the appropriate donor orbital of thymine (the O2 lone-pair orbital of thymine, that is σ_{HOMO-1} or 17σ in Figure 5) is depopulated nor does the C2–H2 antibonding acceptor orbital of adenine (i.e., the σ_{LUMO+2}; not shown in Figure 5) acquire any population. In line with this, the C2–H2 bond distance does not expand but remains unchanged. To get a more quantitative idea on the strength of the C2–H2···O2 interaction, we have analyzed this bond separately from the other bonds, by rotating thymine 180° around an axis through its O2 atom and parallel to the N1–N3 bond (this yields a structure in which both N6–H6···O4 and N1···H3–N3 bonds are broken whereas the C2–H2···O2 moiety is preserved). What we got was a weakly repulsive net interaction energy of only 1.6 kcal mol^{-1}, which arises from +1.0 kcal mol^{-1} electrostatic repulsion, +1.2 kcal mol^{-1} Pauli repulsion and −0.6 kcal mol^{-1} bonding orbital interaction. Thus, we must reject the hypothesis of a stabilizing C–H···O hydrogen bond in AT. This supports Shishkin et al.[10b] who have ruled out C–H···O hydrogen bonding in AT on the basis of a computed (HF/6-31G*) increase of the C–H stretching frequency of adenine in the base pair.

G–C orbital interactions: The MO diagram for GC looks somewhat more complicated than that for AT. This is however not the result of a more complicated bonding mechanism but follows simply from the fact that there are now three instead of only two hydrogen bonds. We find for GC one charge-transfer interactions from G to C, through O6···H4–N4, and two back from C to G, through N1–H1···N3 and N2–H2···O2 (see Scheme 1). The O6···H4–N4 bond is provided by a donor–acceptor interaction between the σ_{HOMO} of guanine, an oxygen O6 lone-pair orbital (21σ in Figure 6) and the lowest
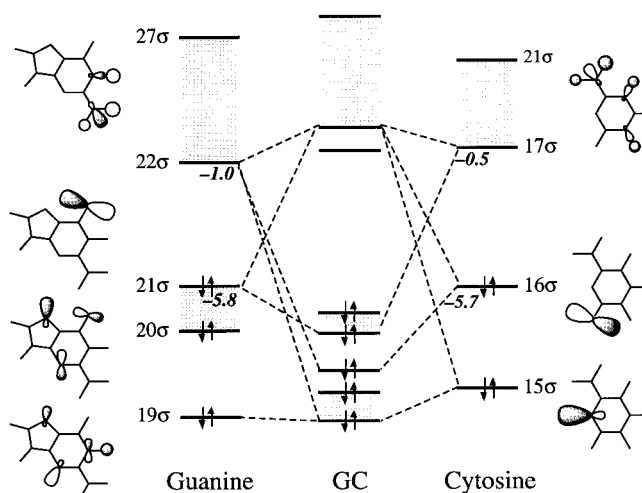

Figure 6. Diagram for the donor–acceptor interactions in the O6···(H)N4, N1(H)···N3 and N2(H)···O2 hydrogen bonds between guanine and cytosine with σ_{HOMO} and σ_{LUMO} energies [eV], obtained at BP86/TZ2P (the lowest unoccupied orbitals that participate in these interactions are represented by a block).

unoccupied N4–H4 antibonding acceptor orbitals on the amino group of cytosine (17σ through 21σ, represented as a block in Figure 6). The resulting bonding combination is split into two levels (i.e., the σ$_{HOMO}$ and σ$_{HOMO-1}$ of the GC pair) as a result of the admixing of the guanine σ$_{HOMO-1}$ (20σ in Figure 6) which does however not contribute to the donor–acceptor interaction. The two N1–H1 ··· N3 and N2–H2 ··· O2 bonds are provided by the donor–acceptor interactions of the cytosine lone-pair orbitals on oxygen O2 (the σ$_{HOMO-1}$, i.e., 15σ) and nitrogen N3 (the σ$_{HOMO}$, i.e., 16σ), respectively, with the lowest unoccupied acceptor orbital of guanine (22σ through 27σ, represented as a block), which are N1–H1 and N2–H2 antibonding (see Figure 6). The bonding combination between cytosine σ$_{HOMO-1}$ and guanine virtuals is split into two levels (i.e., σ$_{HOMO-4}$ and σ$_{HOMO-3}$ of the GC pair, indicated as a block in the MO diagram) as a result of an additional four-electron repulsion that the σ$_{HOMO-1}$ of cytosine (i.e., the 15σ) experiences with the σ$_{HOMO-3}$ of guanine (i.e., the 19σ). The slight elongation of the N–H bonds that participate in hydrogen bonding (see Figure 1) is caused by the donation of charge into the corresponding N–H antibonding σ* orbitals of guanine and cytosine (e.g. 0.05 and 0.02 electrons, respectively, in the corresponding σ$_{LUMO}$'s; not given in Table).

The fact that there are two hydrogen bonds donating charge from C to G and only one donating charge from G to C leads to a net accumulation of negative charge on guanine (−0.03 electrons, Table 5). With the same procedure as for AT (vide supra), the amount of charge-transfer from G to C associated with the individual O6 ··· H4–N4 bond is estimated to be 0.05 electrons (entry 4 in Table 5) which is indeed exceeded by the transfer of 0.07 electrons back from C to G caused by the N1–H1 ··· N3 and N2–H2 ··· O2 bonds together (entry 5 in Table 5; see last section).

Note that, as for AT, as a result of very small overlaps (in the order of 10^{-3}), the π-orbital interactions do not contribute to the net G–C charge transfer ($\Delta Q_{total}^{\pi} = 0$ and $\Delta Q_{total} = \Delta Q_{total}^{\sigma}$, see Table 5). But, again as for AT, the π-electron systems of guanine and cytosine are significantly polarized (mainly a result of the electrostatic potential that the bases experience from each other) leading to a sizeable charge reorganization within each base (see section on charge redistribution).

Quantitative decomposition of the hydrogen bond energy: Now that we know that the DNA bases have suitable charge distributions for electrostatically attracting each other and after having established the occurrence of σ charge transfer and π polarization (see also section on charge redistribution), we want to quantitatively assess the importance of the various components of the A–T and G–C base-pairing energy. Thus, we have carried out a bond-energy decomposition for the Watson–Crick base pairs for two geometries (see Table 6): i) the equilibrium geometry (AT and GC), and ii) a geometry derived from the former by freezing the structures of the individual bases and pulling them 0.1 Å apart along an axis parallel to the hydrogen bonds (AT$_{0.1 Å}$ and GC$_{0.1 Å}$). The latter corresponds to the slightly longer hydrogen bonds observed experimentally in X-ray crystal structure determinations,[1d, 19] and its analysis serves to get an idea if the nature of the

Table 6. Bond-energy decomposition for the Watson–Crick base pairs [kcal mol^{-1}] in the optimized geometry (AT and GC) and with the base–base distance elongated by 0.1 Å (AT$_{0.1 Å}$ and GC$_{0.1 Å}$).[a]

	AT	AT$_{0.1 Å}$	GC	GC$_{0.1 Å}$
Orbital interaction decomposition				
ΔE_{σ}	− 20.7	− 15.9	− 29.3	− 22.8
ΔE_{π}	− 1.7	− 1.3	− 4.8	− 3.9
ΔE_{oi} ($\Delta E_{\sigma} + \Delta E_{\pi}$)	**− 22.4**	**− 17.2**	**− 34.1**	**− 26.7**
Bond-energy decomposition				
ΔE_{Pauli}	39.2	28.6	52.1	37.5
ΔV_{elstat}	− 32.1	− 26.5	− 48.6	− 41.0
$\Delta E_{Pauli} + \Delta V_{elstat}$	**7.1**	**2.1**	**3.5**	**− 3.5**
ΔE_{oi}	− 22.4	− 17.2	− 34.1	− 26.7
ΔE_{int} ($\Delta E_{Pauli} + \Delta V_{elstat} + \Delta E_{oi}$)	− 15.3	− 15.1	− 30.6	− 30.2
ΔE_{prep}	2.3		4.1	
ΔE ($\Delta E_{prep} + \Delta E_{int}$)	− 13.0		− 26.5	

[a] BP86/TZ2P. Bases and base pairs in C_s symmetry.

hydrogen bonds is affected by structural perturbations that may occur in crystals (or under physiological conditions). The orbital interaction is divided into a σ component and a π component. ΔE_{σ} consists mainly of the electron donor–acceptor interactions mentioned above. The π component accounts basically for the polarization in the π system (vide supra) which turns out to partly compensate the local build-up of charge caused by the charge-transfer interactions in the σ system (see section on charge redistribution).

The striking result of our analysis is that charge-transfer orbital interactions are not at all a negligible or minor component in the hydrogen bond energy of Watson–Crick base pairs (see Table 6). Instead, what we find is that charge transfer is of the same order of magnitude as the electrostatic interaction! For AT, ΔE_{oi} is − 22.4 kcal mol^{-1} and ΔV_{elstat} is − 32.1 kcal mol^{-1}, and for GC, ΔE_{oi} is − 34.1 kcal mol^{-1} and ΔV_{elstat} is − 48.6 kcal mol^{-1}. Interestingly, we see that the electrostatic interaction alone is not capable of providing a net bonding interaction; it can only partly compensate the Pauli-repulsive orbital interactions ΔE_{Pauli}. Without the bonding orbital interactions, the net interaction energies of AT and GC at their equilibrium structures would be repulsive by 7.1 and 3.5 kcal mol^{-1}, respectively (Table 6). This parallels the finding of Reed and Weinhold[21] that the water dimer at equilibrium distance would be repulsive without the charge-transfer interactions.

Thus, our analyses disprove the established conception that hydrogen bonding in DNA base pairs is a predominantly electrostatic phenomenon. Almost all arguments we found in the literature in favor of the electrostatic model were eventually based on the work of Umeyama and Morokuma[6] on the hydrogen bond in water dimers and other neutral hydrogen-bound complexes (see Introduction). But in fact, the analyses of Umeyama and Morokuma do reveal a significant charge-transfer component. They[6] found that for the water dimer, for example, the total attractive interaction is provided for 72% by electrostatic interaction, for 21% by charge transfer and for 6% by polarization. We feel that the conclusions of Umeyama and Morokuma are not well represented if this charge-transfer component they found is completely ignored.

In the present work, for both Watson–Crick pairs, that is AT and GC in their equilibrium geometry, we find that ΔE_{oi} provides even 41% of all attractive interactions, while electrostatic forces contribute 59% (Table 6). The ΔE_{oi} can be further split into 38% ΔE_{σ} and 3% ΔE_{π} for AT, and 35% ΔE_{σ} and 6% ΔE_{π} or GC. In the complexes with the 0.1 Å elongated hydrogen bonds, that is $AT_{0.1Å}$ and $GC_{0.1Å}$, ΔE_{oi} provides still 39% of all attractive interactions (Table 6). We conclude that, at variance with current belief, charge transfer plays a vital role in the hydrogen bonds of DNA base pairs.

We were also interested in how the bonding mechanism is affected by more severe changes in the geometry, for example, if the A–T or G–C bond is still further elongated in the way described above for $AT_{0.1Å}$ and $GC_{0.1Å}$ (see also Table 6). Thus, we have analyzed the A–T and G–C bond energy as a function of the base–base distance r; the results are shown in Figures 7 and 8, respectively. Around the equilibrium distance, ΔE_{oi} and ΔV_{elstat} are of the same order of magnitude as discussed above. But at larger hydrogen-bond distances, solely ΔV_{elstat} survives as the only significant term causing attraction. The reason why ΔE_{oi} disappears faster with increasing base–base distance r is that the overlap, necessary for donor–acceptor interactions to occur, vanishes exponentially whereas ΔV_{elstat} decays more slowly as r^{-3}.[13]
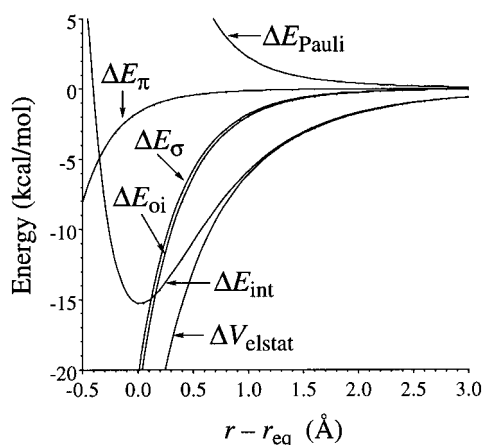

Figure 7. Bond-energy decomposition (at BP86/TZ2P) as function of the adenine–thymine distance ($r - r_{eq} = 0$ corresponds to the equilibrium distance).
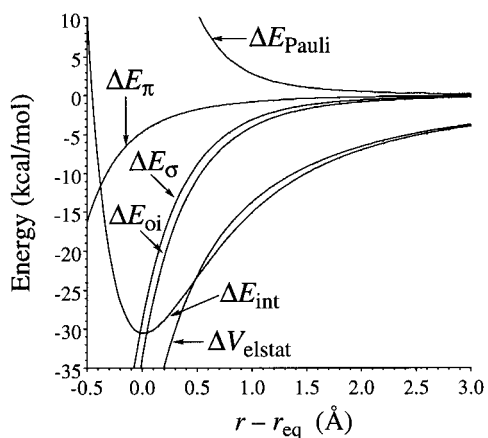

Figure 8. Bond-energy decomposition (at BP86/TZ2P) as function of the guanine–cytosine distance ($r - r_{eq} = 0$ corresponds to the equilibrium distance).

Extension of the VDD method for analyzing the charge distribution

The base-pairing interactions, in particular σ charge transfer and π polarization, discussed in the previous section modify the charge distribution around the nuclei. We have analyzed this reorganization of the charge distribution with the Voronoi deformation density (VDD) method, introduced in ref. [11a]. The VDD charge Q_A^{VDD} of an atom A monitors how much electronic charge moves into ($Q_A^{VDD} < 0$) or out of ($Q_A^{VDD} > 0$) a region of space around nucleus A that is closer to this than to any other nucleus. This particular compartment of space is the Voronoi cell of atom A,[12h] and it is bounded by the bond midplanes on and perpendicular to all bond axes between nucleus A and its neighboring nuclei (cf. the Wigner–Seitz cells in crystals). The VDD charge Q_A^{VDD} is computed as the (numerical) integral of the deformation density $\Delta\rho(\mathbf{r}) = \rho(\mathbf{r}) - \Sigma_B\rho_B(\mathbf{r})$ in the volume of the corresponding Voronoi cell [Eq. (5)].

$$Q_A^{VDD} = - \int_{\substack{Voronoi \\ cell\ of\ A}} (\rho(\mathbf{r}) - \Sigma_B\rho_B(\mathbf{r}))d\mathbf{r} \qquad (5)$$

Here, $\rho(\mathbf{r})$ is the electron density of the molecule and $\Sigma_B\rho_B(\mathbf{r})$ the superposition of atomic densities $\Sigma_B\rho_B(\mathbf{r})$ of a fictitious promolecule without chemical interactions that is associated with the situation in which all atoms are neutral. As has been shown before, the VDD method yields chemically meaningful atomic charges that display hardly any basis set dependence.[11] Note, however, that the value of Q_A^{VDD} does depend on both the chosen reference density (i.e., the promolecule) and the shape of the Voronoi cell.

Front atom problem and its solution: An extension of the VDD method: For the DNA base pairs, we want to know the charge rearrangement associated with the base-pairing interaction, in particular that on the front atoms on each base, that is the atoms pointing toward the other base. It may seem to be a plausible approach to simply compute for each atom A the difference between the atomic charge in the base pair, $Q_{A,pair}^{VDD}$ and that in the separate base, $Q_{A,base}^{VDD}$ [Eq. (6)].

$$\begin{aligned} Q_A^{VDD} &= Q_{A,pair}^{VDD} - Q_{A,base}^{VDD} \\ &= - \left[\int_{\substack{Voronoi\ cell \\ of\ A\ in\ pair}} (\rho_{pair}(\mathbf{r}) - \Sigma_B\rho_B(\mathbf{r}))d\mathbf{r} \right. \\ &\qquad \left. - \int_{\substack{Voronoi\ cell \\ of\ A\ in\ base}} (\rho_{base}(\mathbf{r}) - \Sigma_B\rho_B(\mathbf{r}))d\mathbf{r} \right] \end{aligned} \qquad (6)$$

However, the effect of A–T and G–C hydrogen bonding on the atomic charges is about an order of magnitude smaller than the charge rearrangements due to the primary process of strong chemical bond formation within the individual bases. In that case, Q_A^{VDD} as defined in Equation (6) is not a reliable indicator of the charge flow as a result of hydrogen bonding, at least not for the front atoms that form the bonds with the opposite base. Note that $Q_{A,pair}^{VDD}$ and $Q_{A,base}^{VDD}$ differ in two respects: i) the different molecular densities ρ_{pair} and ρ_{base}, and ii) the altered Voronoi cell. For the front atoms, the latter effect is important since in a free base the Voronoi cell of such

an atom will extend to infinity in the direction where the second base will be located. In the pair, of course, the Voronoi cell of the front atom will have as one of its faces the bond midplane perpendicular to the bond to the other base and cutting that bond in half. This drastic change of the shape of the Voronoi cell has as much effect on the VDD charge as the subtle change of the density from ρ_{base} to ρ_{pair} rendering Equation (6) useless. We wish to emphasize that other methods for the calculation of atomic charges (Mulliken, Hirshfeld, Bader), where the presence of the new neighbor atom in the other base directly affects the atomic charge evaluation on the front atom, are in principle subject to the same kind of problem when the small change in atomic charge as a result of hydrogen bonding is calculated as the difference of the "large" charges in the pair and the base.

The VDD charge analysis offers a natural solution to this problem. The relevant density difference, caused by the hydrogen bonding between the bases, is the difference between the self-consistent field (SCF) density of the pair as final density and the superposition of the densities of the bases as initial density. Integration of this deformation density, which is plotted in Figure 11 (vide infra), over the Voronoi cells of the atoms in the pair will reflect the charge flow due to the hydrogen-bonding interaction [Eq. (7)].

$$\Delta Q_{\text{A}}^{\text{VDD}} = - \int_{\substack{\text{Voronoi cell} \\ \text{of A in pair}}} [\rho_{\text{pair}}(\mathbf{r}) - \rho_{\text{base1}}(\mathbf{r}) - \rho_{\text{base2}}(\mathbf{r})] d\mathbf{r} \qquad (7)$$

The calculation of a small difference of two large numbers that are not completely comparable, as in Equation (6), is now avoided. Only one Voronoi cell is used, the one in the pair, which eliminates the problem identified above. This method for "measuring" the charge rearrangement as a result of the weak hydrogen bonding is of course in the spirit of the VDD calculation of atomic charges resulting from chemical bond formation as in Equation (5) since it integrates the relevant density difference over an appropriate atomic part of space.

Decomposition of VDD charges into σ and π components: To analyze the charge rearrangement caused by charge transfer in the σ system and that caused by polarization in the π system separately, we introduced a further extension of the VDD method: ΔQ_{A} that properly accounts for the effect of base pairing according to Equation (7) is decomposed into the contributions of the σ- and π-deformation densities $\Delta Q_{\text{A}}^{\sigma}$ and $\Delta Q_{\text{A}}^{\pi}$ [Eq. (8)].

$$\Delta Q_{\text{A}}^{\Gamma} = - \int_{\substack{\text{Voronoi cell} \\ \text{of A in pair}}} [\rho_{\text{pair}}^{\Gamma}(\mathbf{r}) - \rho_{\text{base1}}^{\Gamma}(\mathbf{r}) - \rho_{\text{base2}}^{\Gamma}(\mathbf{r})] d\mathbf{r} \qquad (8)$$

The density ρ^{Γ} is obtained as the sum of orbital densities of the occupied molecular orbitals belonging to the irreducible representation Γ [Eq. (9)].

$$\rho^{\Gamma} = \sum_{i \in \Gamma}^{\text{occ}} |\psi_i^{\Gamma}|^2 \qquad (9)$$

Charge redistribution as a result of hydrogen bonding: The changes in atomic charge ΔQ_{A} caused by hydrogen bonding in AT and GC [Eq. (7)] are collected in Figures 9 and 10, respectively. An unexpected pattern emerges for the ΔQ_{A}'s of the atoms directly involved in hydrogen bonds. Instead of

losing density as one would at first expect on the basis of the orbital interactions (see Scheme 2), the electron-donor atoms (oxygen and nitrogen) gain density and become more negative! For AT, we find that adenine N1 and thymine O4 gain negative charges of -0.031 and -0.037 electrons, respectively (Figure 9). Likewise, in GC, the negative charge on guanine O6 increases by -0.049 electrons, and the electron-donor atoms in cytosine, O2 and N3, gain negative charges of -0.030 and -0.037 electrons, respectively (Figure 10). Surprizing is also that the electronic density at the hydrogen atom of the electron-accepting N−H group decreases upon formation of the complex, yielding ΔQ_{A} values ranging from $+0.035$ to $+0.048$ electrons (Figures 9 and 10). An increase of electron density would have been expected as a result of the charge-transfer interactions (see Scheme 2). Furthermore, we only find a moderate accumulation of negative charge on the nitrogen atoms of the electron-accepting N−H groups (Figures 9 and 10).
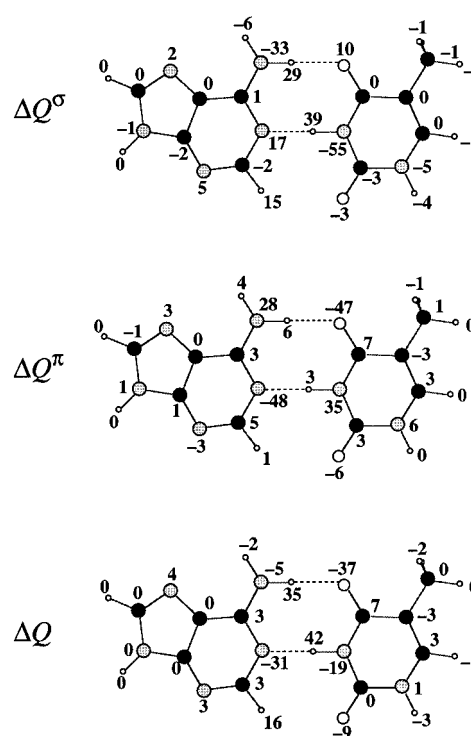

Figure 9. Changes in σ, π and total VDD atomic charges [milli-electrons] on forming the N6(H)···O4 and N1···(H)N3 hydrogen bonds between adenine and thymine in AT (see Scheme 1) calculated at BP86/TZ2P.

How do these ΔQ_{A} values arise or, in other words, what is the physics behind these numbers? We have tried to find out by decomposing ΔQ_{A} into its σ and π components $\Delta Q_{\text{A}}^{\sigma}$ and $\Delta Q_{\text{A}}^{\pi}$ [Eq. (8)] which are also shown in Figures 9 and 10. The $\Delta Q_{\text{A}}^{\sigma}$ values reveal a clear charge-transfer picture for AT and GC: Negative charge is lost on the electron-donor atoms whereas there is a significant accumulation of negative charge on the nitrogen atoms of the electron-accepting N−H bonds. It is the reorganization of charge stemming from π polarization, as reflected by the $\Delta Q_{\text{A}}^{\pi}$ values, that causes the counter-intuitive pattern of the overall charge rearrangement monitored by ΔQ_{A}. Note that $\Delta Q_{\text{A}}^{\sigma}$ and $\Delta Q_{\text{A}}^{\pi}$ are of the same order
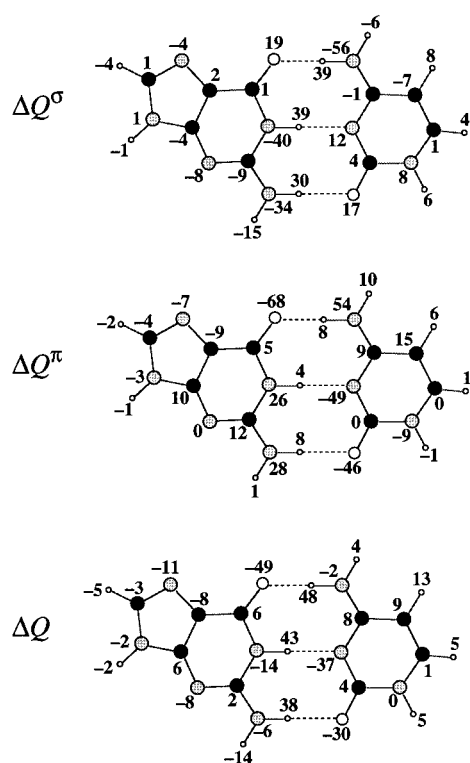
Figure 10. Changes in σ, π and total VDD atomic charges [mili-electrons] on forming the O6···(H)N4, N1(H)···N3 and N2(H)···O2 hydrogen bonds between guanine and cytosine in GC (see Scheme 1) calculated at BP86/TZ2P.
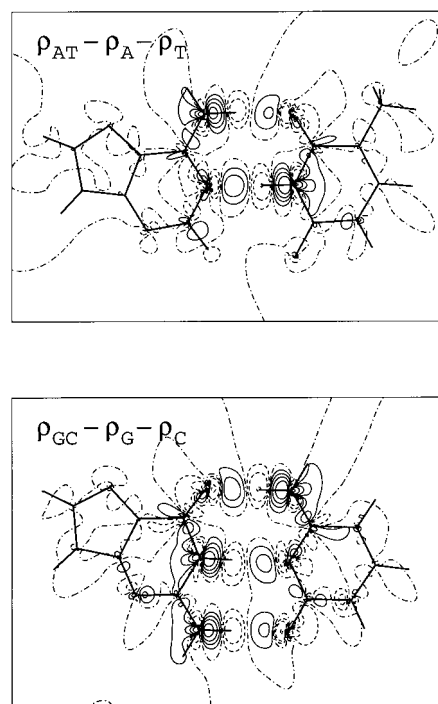

Figure 11. Contour plots for AT and GC of the difference between the density of the base pair and the superposition of densities of the individual bases calculated at BP86/TZ2P (Scan values: ± 0.05, ± 0.02, ± 0.01, ± 0.005, ± 0.002, 0. Solid, dashed and dash-dotted contours indicate positive, negative and zero values, respectively).

of magnitude whereas ΔE_π is an order of magnitude smaller than ΔE_σ (see section on nature of the hydrogen bond). The π-electron density of the bases is polarized in such a way that the build-up of charge arising from charge-transfer interactions in the σ system is counteracted and compensated: The electron-donor atoms gain π density and the nitrogen atoms of the electron-accepting N–H bonds loose π density (compare ΔQ_A^σ and ΔQ_A^π in Figures 9 and 10). This suggests that there may be some kind of cooperativity between the σ charge transfer and π polarization which is reminiscent of the resonance assistance proposed by Gilli et al.[7a] In the following section, we examine if such a synergism between ΔE_σ and ΔE_π interactions really exists.

But first we want to resolve the still open question why hydrogen bonding makes the hydrogen atoms involved more positive (Figures 9 and 10). This turns out to be a subtle mechanism. To get an idea how the positive ΔQ_A charges of these hydrogen atoms arise, we have plotted the corresponding deformation densities for the formation of AT and GC from their separate bases (i.e., the density of the base pair minus the superimposed densities of the bases) in Figure 11. These deformation-density plots nicely show the depletion of charge around the hydrogen-bonding hydrogen atoms that the VDD charges had already detected. A more detailed examination reveals that an important portion of this charge depletion stems from the Pauli repulsion (i.e., ΔE_{Pauli}) between the occupied orbitals of the two bases, in particular the strongly overlapping O or N lone pairs of one base and the occupied N–H σ-bonding orbitals of the other base. But also the bonding orbital interactions (i.e., ΔE_{oi}) contribute to this

feature in the deformation density. Morokuma and co-workers[6b,c] have ascribed the charge depletion around the hydrogen-bonding hydrogen atom in, for example, the water dimer to a large extent to polarization in the σ-electron system even though this term appears to contribute only little to the interaction energy. A further mechanism that may contribute to the depletion of charge around these hydrogen atoms is that the lone pairs that donate charge, penetrate deeply into the space around the hydrogen nucleus of the partner N–H bond, that is the Voronoi cell of that hydrogen atom. Consequently, as the lone pair gets depopulated during charge transfer, it causes a depletion of charge not only on the donor atom but also in the Voronoi cell of the "accepting" hydrogen atom. Meanwhile, the N–H acceptor orbitals have a compact high amplitude character around the nitrogen atom whereas they are more extended and diffuse on hydrogen (see Figures 3 and 4). This makes that the electronic charge accepted during charge transfer appears in a region closely around the nucleus of nitrogen and more distant from that of hydrogen. Thus, we find that thanks to the two extensions presented here the VDD method has become a valuable tool for monitoring and analyzing even very subtle charge rearrangements.

Synergism in hydrogen bonding

At this point, we are left with three questions concerning DNA base pairing: i) Do the hydrogen bonds that donate charge in opposite directions reinforce each other by reducing the net build-up of charge on each base? ii) Is there a cooperative effect or resonance assistance by the π-electron system as suggested by Gilli et al.?[7a] and iii) How important

is π polarization for the hydrogen-bonding structure (i.e., bond distances)? To answer these questions, we have carried out further detailed analyses of the base-pairing energies, in which individual types of orbital interactions are considered while others are switched off by removing the appropriate σ or π virtuals from the respective DNA bases. The results are collected in Tables 7 and 8. Our notation is exemplified for the AT pair: A(σ,π)T(σ,π) corresponds to a regular computation on AT in which all σ and π virtuals are included; A(σ, −)-T(σ, −), for example, indicates that all σ virtuals are available on A and T whereas the π virtuals have been removed from both bases.

Table 7. Analysis of the synergy between σ- and π-orbital interactions in A – T [kcal mol^{-1}].[a]

		Virtuals available[b]	ΔE_σ	ΔE_π	ΔE_{oi}
I		A(σ,π)T(σ,π)	− 20.7	− 1.7	− 22.4
II	**a**	A(−,−)T(σ,−)	− 12.9		
	b	A(σ,−)T(−,−)	− 8.3		
	a + b		**− 21.2**		
	c	A(−,−)T(−,π)		− 0.7	
	d	A(−,π)T(−,−)		− 0.7	
	c + d			**− 1.4**	
III	**a**	A(σ,−)T(σ,−)	− 20.4		− 20.4
	b	A(−,π)T(−,π)		− 1.3	− 1.3
	a + b				**− 21.7**

[a] BP86/TZ2P. [b] A(σ, −)T(σ, −) for example indicates: σ virtuals available on and π virtuals removed from both A and T.

Table 8. Analysis of the synergy between σ- and π-orbital interactions in G – C [kcal mol^{-1}].[a]

		Virtuals available[b]	ΔE_σ	ΔE_π	ΔE_{oi}
I		G(σ,π)C(σ,π)	− 29.3	− 4.8	− 34.1
II	**a**	G(−,−)C(σ,−)	− 13.6		
	b	G(σ,−)C(−,−)	− 16.4		
	a + b		**− 30.0**		
	c	G(−,−)C(−,π)		− 2.0	
	d	G(−,π)C(−,−)		− 1.6	
	c + d			**− 3.6**	
III	**a**	G(σ,−)C(σ,−)	− 28.9		− 28.9
	b	G(−,π)C(−,π)		− 3.8	− 3.8
	a + b				**− 32.7**

[a] BP86/TZ2P. [b] G(σ, −)C(σ, −) for example indicates: σ virtuals available on and π virtuals removed from both G and C.

Synergism between individual hydrogen bonds in DNA base pairs? The synergism within the σ system between charge transfer from one base to the other through one hydrogen bond and back through the other hydrogen bond (AT) or bonds (GC) is obtained as the difference between ΔE_σ in entry IIIa and entry IIa + b in Table 7 or 8. In IIIa, charge-transfer interactions in both directions occurs simultaneously, whereas IIa + b gives the sum of the situations with charge-transfer interaction forth only and back only; π polarization is completely switched off. The anticipated synergic effect does not occur: We find that ΔE_σ(IIIa) − ΔE_σ(IIa + b) is close to zero with values of + 0.8 and + 1.1 kcal mol^{-1} for AT and GC (see Tables 7 and 8). This suggests that the hydrogen bonds donating charge in opposite directions operate independently. This is nicely confirmed by comparing the regular deforma-

tion density (e.g. $\Delta\rho_{AT} = \rho_{AT} - \rho_A - \rho_T$, see Figure 11) with the deformation densities belonging to IIa and IIb (i.e., $\Delta\rho_{A(\sigma,-)T(--)} = \rho_{A(\sigma,-)T(--)} - \rho_A - \rho_T$ and $\Delta\rho_{A(-,-)T(\sigma-)} = \rho_{A(-,-)T(\sigma-)} - \rho_A - \rho_T$ not shown in Figure). This comparison shows that the charge-transfer processes that donate charge in opposite directions do not affect each others locally induced (and conversely oriented) charge separations, while their simultaneous occurrence still does reduce the net build-up of charge. The fact that ΔE_σ(III) − ΔE_σ(IIa + b) is even slightly destabilizing can be ascribed to the repulsion accompanying the simultaneous occurrence in III but not in IIa or IIb of an accumulation of density both at the donor and acceptor atoms next to each other on the same base (see Figure 11).

In the same manner, we can compute the synergism between the π polarizations occurring on each of the bases as the difference between ΔE_π in entry IIIb and entry IIc + d in Table 7 or 8. In IIIb, π polarization occurs on both bases simultaneously, whereas IIc + d gives the sum of the situations with π polarization on one base only and on the other base only; charge transfer in the σ-electron system is completely switched off. Again, there is no synergic effect with ΔE_π(IIIb) − ΔE_π(IIc + d) being virtually zero (0.1 and 0.2 kcal mol^{-1} for AT and GC). Thus, the π polarizations occurring in each individual base of a base pair are independent.

Synergism between σ charge transfer and π polarization? The synergism between charge transfer in the σ-electron system (ΔE_σ) and polarization in the π-electron system (ΔE_π) can be computed as the difference between ΔE_{oi} in entry I and entry IIIa + b in Tables 7 or 8. In I, all σ charge transfer and π polarization interactions occur simultaneously, whereas IIIa + b gives the sum of the situations in which there is σ charge transfer interaction only and π polarization only. We find very small synergic effects ΔE_{oi}(I) − ΔE_{oi}(IIIa + b) of − 0.7 and − 1.4 kcal mol^{-1} for AT and GC. The overall synergic effect is composed of a synergic stabilization in the σ charge transfer interaction ΔE_σ(I) − ΔE_σ(IIIa) of − 0.3 and − 0.4 kcal mol^{-1}, and a synergic stabilization in the π polarization ΔE_π(I) − ΔE_π(IIIa) of − 0.4 and − 1.0 kcal mol^{-1} for AT and GC, respectively.

We conclude that the π electrons give almost no assistance to the donor – acceptor interactions in the hydrogen bonds in the sense of a synergism. Energetically, the main assistance caused by the π electrons is simply the small although not negligible term ΔE_π which contributes − 1.7 and − 4.8 kcal mol^{-1} to the net hydrogen bond energy (see Tables 3, 4, 7 and 8; see also section on nature of the hydrogen bond).

But how important is this ΔE_π term for the structure, that is, the hydrogen-bond distances of the DNA base pairs? We can determine this influence, by computing the bond energy with π polarization switched on and off (i.e., with or without the π virtuals of the bases) as a function of the base – base distance (we follow the procedure for varying the bond length described before in section on nature of the hydrogen bond). The resulting bond energy curves are shown in Figure 12.

The comparison between the curves of A(σ,π)T(σ,π) and G(σ,π)C(σ,π) (i.e., π polarization switched on) and those of
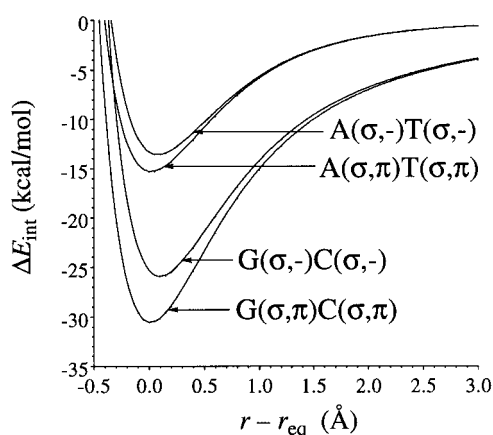
Figure 12. Interaction energy of AT and GC with and without πvirtuals as function of the base-base distance calculated at BP86/TZ2P ($r - r_{eq} = 0$ corresponds to the equilibrium distance).

$A(\sigma, -)T(\sigma, -)$ and $G(\sigma, -)C(\sigma, -)$ (i.e., π polarization off) shows that without π polarization the equilibrium hydrogen-bond distances expand for both base pairs by some 0.1 Å. This would yield hydrogen-bond lengths for AT of 2.95 and 2.91 Å and for GC of 2.97, 2.98 and 2.83 Å. One might conceive the extra bond shortening caused by π polarization as some kind of resonance assistance. However, we stress again that ΔE_π is only a minor bonding component and that there is no resonance-assistance in the sense of a synergism between σ-charge transfer and π polarization.

Conclusions

The hydrogen bond in DNA base pairs is, at variance with widespread belief, not a pure or essentially electrostatic phenomenon. Instead, as follows from our BP86/TZ2P investigation, it has a substantial charge-transfer character caused by donor–acceptor orbital interactions (between O or N lone pairs and N−H σ*-acceptor orbitals) that are of the same order of magnitude as the electrostatic term. Polarization in the π-electron system provides an additional stabilizing term. This is, however, one order of magnitude smaller than the σ donor–acceptor interactions. It still has the effect of reducing the base–base bond distance by 0.1 Å. A more detailed bond analysis shows that no substantial synergism occurs between the individual hydrogen bonds in the base pairs nor between σ orbital interactions and π polarization. And there is no C−H···O hydrogen bond in AT. The occurrence of charge transfer and polarization in the σ- and π-electron system, respectively, is confirmed by our complementary analysis of the electron density distribution with the extensions of the VDD method that we have introduced in the present work.

It is evident that many other factors are of great importance for the working of the molecular genetic machinery (e.g., structural complementarity of bases, hydrophobic interactions and other medium effects, interaction with enzymes and other proteins, etc.).[1d, 22] However, regarding the intrinsic cohesion of DNA, we may conclude that it is the chemical charge-transfer nature of the hydrogen bond in Watson–Crick base pairs, rather than resonance assistance by the π-electron system, that together with the classical electrostatic interaction is vital to the behavior and the stability and, thus, the evolution of nature's genetic code.

[1] a) G. A. Jeffrey, W. Saenger, *Hydrogen Bonding in Biological Structures*, Springer, Berlin, **1991**; b) G. A. Jeffrey, *An Introduction to Hydrogen Bonding*, Oxford University Press, New York, **1997**, Chapter 10; c) J. D. Watson, F. H. C. Crick, *Nature* **1953**, *171*, 737; d) W. Saenger, *Principles of Nucleic Acid Structure*, Springer, New York, **1984**.

[2] a) J. P. Lewis, O. F. Sankey, *Biophys. J.* **1995**, *69*, 1068; b) Y. S. Kong, M. S. Jhon, P. O. Löwdin, *Int. J. Quantum. Chem. Symp. QB* **1987**, *14*, 189; c) C. Nagata, M. Aida, *J. Mol. Struct.* **1988**, *179*, 451; d) I. R. Gould, P. A. Kollman, *J. Am. Chem. Soc.* **1994**, *116*, 2493; e) J. Sponer, J. Leszczynski, P. Hobza, *J. Phys. Chem.* **1996**, *100*, 1965; f) J. Sponer, J. Leszczynski, P. Hobza, *J. Biomol. Struct. Dyn.* **1996**, *14*, 117; g) J. Sponer, P. Hobza, J. Leszczynski, in *Computational Chemistry. Reviews of Current Trends* (Ed.: J. Leszczynski), World Scientific Publisher, Singapore, **1996**, p. 185–218; h) M. Hutter, T. Clark, *J. Am. Chem. Soc.* **1996**, *118*, 7574; i) K. Brameld, S. Dasgupta, W. A. Goddard III, *J. Phys. Chem. B* **1997**, *101*, 4851; j) M. Meyer, J. Sühnel, *J. Biomol. Struct. Dyn.* **1997**, *15*, 619; k) R. Santamaria, A. Vázquez, *J. Comp. Chem.* **1994**, *15*, 981; l) J. Bertran, A. Oliva, L. Rodríguez-Santiago, M. Sodupe, *J. Am. Chem. Soc.* **1998**, *120*, 8159.

[3] a) F. Sim, A. St-Amant, I. Papai, D. R. Salahub, *J. Am. Chem. Soc.* **1992**, *114*, 4391; b) H. Guo, S. Sirois, E. I. Proynov, D. R. Salahub, in *Theoretical Treatment of Hydrogen Bonding* (Ed.: D. Hadzi), Wiley, New York, **1997**; c) S. Sirois, E. I. Proynov, D. T. Nguyen, D. R. Salahub, *J. Chem. Phys.* **1997**, *107*, 6770; d) P. R. Rablen, J. W. Lockman, W. L. Jorgensen, *J. Phys. Chem.* **1998**, *102*, 3782; e) K. Kim, K. D. Jordan, *J. Phys. Chem.* **1994**, *98*, 10089; f) J. J. Novoa, C. Sosa, *J. Phys. Chem.* **1995**, *99*, 15837; g) Z. Latajka, Y. Bouteiller, *J. Chem. Phys.* **1994**, *101*, 9793; h) J. E. Del Bene, W. B. Person, K. Szczepaniak, *J. Phys. Chem.* **1995**, *99*, 10705; i) J. Florian, B. G. Johnson, *J. Phys. Chem.* **1995**, *99*, 5899; j) J. E. Combariza, N. R. Kestner, *J. Phys. Chem.* **1995**, *99*, 2717; k) B. Civalleri, E. Garrone, P. Ugliengo, *J. Mol. Struct.* **1997**, *419*, 227; l) M. Lozynski, D. Rusinska-Roszak, H.-G. Mack, *J. Phys. Chem.* **1998**, *102*, 2899; m) A. K. Chandra, M. Nguyen, *Chem. Phys.* **1998**, *232*, 299; n) B. Paizs, S. Suhai, *J. Comp. Chem.* **1998**, *19*, 575; o) M. A. McAllister, *J. Mol. Struct.* **1998**, *427*, 39; p) Y. P. Pan, M. A. McAllister, *J. Mol. Struct.* **1998**, *427*, 221; q) L. Gonzalez, O. Mo, M. Yanez, *J. Comp. Chem.* **1997**, *18*, 1124.

[4] C. Fonseca Guerra, F. M. Bickelhaupt, *Angew. Chem.* **1999**, *111*, 3120; *Angew. Chem. Int. Ed.* **1999**, *38*, 2942.

[5] C. Fonseca Guerra, F. M. Bickelhaupt, J. G. Snijders, E. J. Baerends, submitted.

[6] a) H. Umeyama, K. Morokuma, *J. Am. Chem. Soc.* **1977**, *99*, 1316; b) S. Yamabe, K. Morokuma, *J. Am. Chem. Soc.* **1975**, *97*, 4458; c) K. Morokuma, *Acc. Chem. Res.* **1977**, *10*, 294.

[7] a) G. Gilli, F. Bellucci, V. Ferretti, V. Bertolasi, *J. Am. Chem. Soc.* **1989**, *111*, 1023; b) P. Gilli, V. Ferretti, V. Bertolasi, G. Gilli, *Adv. Mol. Struct. Res.* **1996**, *2*, 67–102; c) G. Gilli, V. Bertolasi, V. Ferretti, P. Gilli, *Acta Crystallogr. Sect. B* **1993**, *49*, 564; d) V. Bertolasi, P. Gilli, V. Ferretti, G. Gilli, *Acta Crystallogr. Sect. B* **1995**, *51*, 1004.

[8] M. L. Huggins, *Angew. Chem.* **1971**, *83*, 163; *Angew. Chem. Int. Ed. Engl.* **1971**, *10*, 147.

[9] a) F. M. Bickelhaupt, E. J. Baerends, *Rev. Comput. Chem.*, submitted; b) R. Hoffmann, *Angew. Chem.* **1982**, *94*, 725; *Angew. Chem. Int. Ed.*

Engl. **1982**, *21*, 711; c) T. A. Albright, J. K. Burdett, M. Whangbo, *Orbital Interactions in Chemistry*, Wiley, New York, **1985**; d) B. Gimarc, *The Qualitative Molecular Orbital Approach*, Academic Press, New York, **1979**.

[10] C−H ⋯ O Hydrogen bonding in AT has been suggested by: a) G. A. Leonard, K. McAuley-Hecht, T. Brown, W. N. Hunter, *Acta Crystallogr. Sect. D* **1995**, *51*, 136. It has been ruled out for AT by: b) O. V. Shishkin, J. Sponer, P. Hobza, *J. Mol. Struct.* **1999**, *477*, 15. For studies that do find C−H ⋯ O hydrogen bonding in other systems, see, for example: c) K. N. Houk, S. Menzer, S. P. Newton, F. M. Raymo, J. F. Stoddart, D. J. Williams, *J. Am. Chem. Soc.* **1999**, *121*, 1479; d) P. Seiler, G. R. Weisman, E. D. Glendening, F. Weinhold, V. B. Johnson, J. D. Dunitz, *Angew. Chem.* **1987**, *99*, 1216; *Angew. Chem. Int. Ed. Engl.* **1987**, *26*, 1175.

[11] a) F. M. Bickelhaupt, N. J. R. van Eikema Hommes, C. Fonseca Guerra, E. J. Baerends, *Organometallics* **1996**, *15*, 2923; b) F. M. Bickelhaupt, C. Fonseca Guerra, J.-W. Handgraaf, E. J. Baerends, unpublished results.

[12] a) C. Fonseca Guerra, O. Visser, J. G. Snijders, G. te Velde, E. J. Baerends, in *Methods and Techniques for Computational Chemistry* (Eds.: E. Clementi, G. Corongiu), STEF, Cagliari **1995**, p. 305 – 395; b) E. J. Baerends, D. E. Ellis, P. Ros, *Chem. Phys.* **1973**, *2*, 41; c) E. J. Baerends, P. Ros, *Chem. Phys.* **1975**, *8*, 412; d) E. J. Baerends, P. Ros, *Int. J. Quantum Chem. Symp., Quantum Chem.* **1978**, *12*, 169; e) W. Ravenek, in *Algorithms and Applications on Vector and Parallel Computers* (Eds.: H. H. J. Riele, T. J. Dekker, H. A. van de Vorst), Elsevier, Amsterdam, **1987**; f) C. Fonseca Guerra, J. G. Snijders, G. te Velde, E. J. Baerends, *Theor. Chem. Acc.* **1998**, *99*, 391; g) P. M. Boerrigter, G. te Velde, E. J. Baerends, *Int. J. Quantum Chem.* **1988**, *33*, 87; h) G. te Velde, E. J. Baerends, *J. Comp. Phys.* **1992**, *99*, 84; i) J. G. Snijders, E. J. Baerends, P. Vernooijs, *At. Nucl. Data Tables* **1982**, *26*, 483; j) J. Krijn, E. J. Baerends, *Fit-Functions in the HFS-Method; Internal Report (in Dutch)*, Vrije Universiteit, Amsterdam, **1984**; k) L. Versluis, T. Ziegler, *J. Chem. Phys.* **1988**, *88*, 322; l) L. Fan, L. Versluis, T. Ziegler, E. J. Baerends, W. Ravenek, *Int. J. Quantum. Chem. Quantum Chem. Symp.* **1988**, *S22*, 173; m) J. C. Slater, *Quantum Theory of Molecules and Solids, Vol. 4*, McGraw-Hill, New York, **1974**; n) A. D. Becke, *J. Chem. Phys.* **1986**, *84*, 4524; o) A. Becke, *Phys. Rev. A* **1988**, *38*, 3098; p) S. H. Vosko, L. Wilk, M. Nusair, *Can. J. Phys.* **1980**, *58*, 1200; q) J. P. Perdew, *Phys. Rev. B* **1986**, *33*, 8822; Erratum: *Phys. Rev. B* **1986**, *34*, 7406); r) L. Fan, T. Ziegler, *J. Chem. Phys.* **1991**, *94*, 6057; s) T. Ziegler, *Chem. Rev.* **1991**, *91*, 651.

[13] P. W. Atkins, *Physical Chemistry*, Oxford University Press, Oxford, **1998**.

[14] S. F. Boys, F. Bernardi, *Mol. Phys.* **1970**, *19*, 553.

[15] a) F. M. Bickelhaupt, N. M. M. Nibbering, E. M. van Wezenbeek, E. J. Baerends, *J. Phys. Chem.* **1992**, *96*, 4864; b) T. Ziegler, A. Rauk, *Inorg. Chem.* **1979**, *18*, 1755; c) T. Ziegler, A. Rauk, *Inorg. Chem.* **1979**, *18*, 1558; d) T. Ziegler, A. Rauk, *Theor. Chim. Acta* **1977**, *46*, 1.

[16] a) J. P. Perdew, in *Electronic Structure of Solids* (Eds.: P. Ziesche, H. Eschrig), Akademie Verlag, Berlin, **1991**, p. 11 – 20; b) J. P. Perdew, J. A. Chevary, S. H. Vosko, K. A. Jackson, M. R. Pederson, D. J. Singh, C. Fiolhais, *Phys. Rev. B* **1992**, *46*, 6671.

[17] a) C. Lee, W. Yang, R. G. Parr, *Phys. Rev. B* **1988**, *37*, 785; b) B. G. Johnson, P. M. W. Gill, J. A. Pople, *J. Chem. Phys.* **1992**, *98*, 5612.

[18] I. K. Yanson, A. B. Teplitsky, L. F. Sukhodub, *Biopolymers* **1979**, *18*, 1149.

[19] a) N. C. Seeman, J. M. Rosenberg, F. L. Suddath, J. J. P. Kim, A. Rich, *J. Mol. Biol.* **1976**, *104*, 109 – 144; b) J. M. Rosenberg, N. C. Seeman, R. O. Day, A. Rich, *J. Mol. Biol.* **1976**, *104*, 145.

[20] The role of structural complementarity for Watson – Crick base pairing is discussed, for example, in: a) S. Moran, R. X.-F. Ren, S. Rumney, E. T. Kool, *J. Am. Chem. Soc.* **1997**, *119*, 2056; b) U. Diederichsen, *Angew. Chem.* **1998**, *110*, 2056; *Angew. Chem. Int. Ed.* **1998**, *37*, 1655. See, however, also: c) T. A. Evans, K. R. Seddon, *Chem. Commun.* **1997**, 2023. For a very recent discussion of the role of minor groove interactions between DNA and polymerase for replication, see: d) J. C. Morales, E. T. Kool, *J. Am. Chem. Soc.* **1999**, *121*, 2323.

[21] a) A. E. Reed, F. Weinhold, *J. Chem. Phys.* **1983**, *78*, 4066. See also: b) A. E. Reed, F. Weinhold, L. A. Curtiss, D. J. Pochatko, *J. Chem. Phys.* **1986**, *84*, 5687; c) L. A. Curtiss, D. J. Pochatko, A. E. Reed, F. Weinhold, *J. Chem. Phys.* **1985**, *82*, 2679.

[22] a) L. Stryer, *Biochemistry*, W. H. Freeman, New York, **1988**; b) M. W. Strickberger, *Evolution*, Jones and Bartlett, Boston, **1996**, Chapters 7 and 8; c) A. Kornberg, T. A. Baker, *DNA Replication*, Freeman, New York, **1992**.